Causal Dynamical Triangulation of Quantum Gravity in Three Dimensions

J. Z. Zhang *

Cornell University

August 29, 2007

Abstract

The theory of causal dynamical triangulation in (2+1) dimensions is studied through the help of Monte Carlo simulations. The basic ideas behind this particular approach to quantum gravity are outlined in the paper. The numerical setup and the results from the simulations are presented and discussed. Based on the numerical results, the theory is shown to possess a non-trivial classical limit. The effective dimension of the emergent quantum universe is examined by means of measurements of the fractal spectral dimension.

1 Introduction

Formulating a consistent quantum theory of gravity lies at the root of our understanding of nature and still remains as one of the greatest challenges in theoretical physics today. In recent years, a particular discrete approach to quantum gravity called the causal dynamical triangulation or CDT in short, invented by Loll, Ambjorn, and Jurkiewicz, has received considerable attention. The CDT approach defines quantum gravity through nonperturbative state sums of causally triangulated geometries, and is particularly expedient for numerical implementations. Numerical simulations in both 3 and 4 dimensions have yielded promising results indicating a non-trivial micro-structure of spacetime geometry governed by quantum laws and a semi-classical behavior of the theory in the large-scale limits [1, 2, 3]. We have developed a computer

---

*jzz3@cornell.edu.

program to simulate the model in 3 dimensions, in hope of confirming some of the results obtained by Loll etc. as well as discovering other new interesting insights for quantum gravity in 3 dimensions. In this paper, we will briefly describe this novel approach to quantizing gravity and discuss some of the results we obtained in our computer simulations.

2   Quantum Gravity

Gravity in classical general relativity [4] is described by a symmetric tensor field $g_{\mu\nu}(x)$ with a Lorentzian signature called the metric which determines locally the values of distances and angle measurements in spacetime. The theory is intrinsically geometric in the sense that the spacetime is represented by a smooth manifold M with measurable quantities (the metric, particle velocity, electromagnetic field, etc.) being tensor fields defined on the manifold. This property of general relativity is referred to as general covariance or diffeomorphic invariance. The metric tensor $g_{\mu\nu}(x)$ satisfies the Einstein's equations with the energy and matter distribution in the spacetime serving as the source term in these equations.

Quantum mechanics on the other hand describes the state of a physical system mathematically as a vector in a Hilbert space (or a product of a set of Hilbert spaces in the case of quantum field theory). In Feynman's path integral formulation of quantum mechanics [5], the quantum amplitude (inner product of two state vectors) of a process is given by a sum over all histories, or all possible configurations that connects the two states, each of which is weighted by e^{-iS}, where S is the action of that history. Ordinary quantum field theory describes the dynamics of elementary particles and their interactions on a fixed spacetime background, usually that of the flat Minkowski space of special relativity.

Both theories work extraordinarily well at the scales for which they are valid. However, the task of unifying the two theories under one theoretical framework is a notoriously difficult one. The difficulties of finding a consistent theory of quantum gravity are on the one hand due to the lack of experimental tests and further complicated by the fact that the two theories make drastically different assumptions on how nature works. General relativity is a nonlinear theory and is thus intrinsically more complicated than linear field theories such as electrodynamics. Moreover, the theory is nonrenormalizable so applying the usual perturbative quantum field theoretic methods fails to produce a sensible theory of quantum gravity. General relativity is a theory of that describes the dynamics of the geometry of spacetime, which at the same time, serves

as a playground for other matter fields. Therefore, quantizing gravity means quantizing spacetime itself.

3   Causal Dynamical Triangulation

In this section, we attempt to give a rough summary of the theory of CDT. For a more thorough introduction, the read is referred to [6].

The approach of CDT follows a minimalist spirit in the sense that it is based on a minimal set of well-known physical principles and tools such as quantum superposition, triangulation of geometry, and etc. The theory is both background independent and nonperturbative, by which we mean that the theory does not simply describe the dynamics of gravity as linear perturbation around some preferred background metric.

To simplify the problem, we will from now on assume that we can break up the spatial and temporal parts of our spacetime, i.e., the spacetime under consideration has the topology $[0, 1] \times \Sigma$, where Σ represents a compact spatial hypersurface. In other words, we can choose a global time function t such that each surface of constant t is a spatial Cauchy surface.

Gravitational Path Integral

In CDT, quantization is carried out through the path integral:

$$G(\mathbf{g}_0, \mathbf{g}_1; t_0, t_1) = \int \mathcal{D}g \, e^{iS_{\mathrm{EH}}[g]} \,, \tag{1}$$

where

$$S_{\mathrm{EH}}[g] = \frac{1}{16\pi G} \int d^n x \sqrt{-g}(R - 2\Lambda) \tag{2}$$

is the usual Einstein-Hilbert action for gravitation, the variational equations of which are the Einstein's equations. Here g denotes the spacetime metric that interpolates between the two spatial metrics $\mathbf{g}_0$ and $\mathbf{g}_1$. General relativity is taken to be an ordinary field theory with the metric $g_{\mu\nu}$ representing its field degrees of freedom which are to be integrated over in the path integral to produce a quantum theory.

Let us discuss briefly what it means by a gravitational path integral and address some related issues. Analogous to the usual interpretation of the path integral, the propagator G here is given by a superposition of all virtual space-times, each of which is weighted by the classical action. In contrast to the usual path integral formulation of quantum mechanics and quantum field theory, the

gravitational path integral is more intricate due to the diffeomorphism invariance of the theory and due to the absence of a preferred background metric. Due to the diffeomorphism invariance, the path integral (1) should be taken over the space of all geometries rather than the space of all metrics because any two metrics are equivalent if they can be mapped onto each other by a coordinate transformation, in other words, the functional measure $\mathcal{D}g$ must be defined in a covariant way. Because there is no obvious way to parametrize geometries, one may suggest that we introduce covariant metric tensor as a field variable to evaluate the integral. However, this leads to the complication that gauge fixing the metric tensor using techniques such as the Faddeev-Popov determinants requires exceedingly difficult nonperturbative evaluation.

The path integral as it stands is not mathematically well-defined. In ordinary quantum field theory, to actually evaluate the integral one usually performs a Wick rotation by analytically continuing the time variable t to the imaginary axis, i.e., $t \mapsto it$. The Wick rotation converts a problem in Lorentzian spacetime M_{Lor} to one in Euclidean space M_{Euc}. It is not obvious how the Wick rotation needs to be carried out in the gravitational setting. The ad hoc substitution $iS_{\text{Lor}} \to -S_{\text{Euc}}$ that is used widely in field theories is in fact the basis for the predecessor of CDT, the Euclidean dynamical triangulation [7]. As will be discussed shortly, CDT is based on a different program for carrying out the Wick rotation, one that specifically preserves the causality of spacetime, setting it apart from the old Euclidean approach.

Regge Calculus

To perform the calculation nonperturbatively, we use a lattice method similar to those used in lattice gauge theories. In the field theoretic context, the lattice spacing a will naturally serve as a cutoff of the theory. The continuum limit is extracted by taking the lattice spacing a to zero and hoping that the resulting theory is independent of the cutoff. This suggests that we need some specific scheme for discretization of spacetime geometries. The idea of approximating a spacetime manifold by a piecewise flat spacetime was first developed by Regge [8] and is called the Regge calculus which has been successfully applied in numerical general relativity and quantum gravity before CDT [9].

Instead of considering spaces with smooth curvature, Regge looked at spaces where the curvature is restricted to subspaces of codimension two, based on the division of the manifold into elementary building blocks which are usually taken to be simplices, i.e., higher dimensional analogs of triangles, with consistent edge length assignments l_i. For example, a simplex in two dimensions is a flat triangle and in three dimensions a tetrahedron, and so on. A

4

simplicial manifold or equivalently a triangulation of a smooth manifold is obtained by gluing together these simplicial building blocks in an appropriate manner. The Einstein-Hilbert action can then be written as a functional of the edge lengths only, by making the following substitutions [10]:

$$\int d^n x \sqrt{-g} R \ \rightarrow \ 2 \sum_{j \in T} \epsilon_j \,, \tag{3}$$

$$\int d^n x \sqrt{-g} \ \rightarrow \ \sum_{j \in T} V_j \,, \tag{4}$$

where j is an index labeling the hinges, i.e., the elements of codimension two (points in 2D, edges in 3D, triangular faces in 4D, and etc.) where curvature resides in a particular triangulation T. ϵ_j is the so-called deficit angle and V_j the dual volume of the hinge j. In terms of these geometric variables, the action (2) is written as

$$S_{\text{Regge}}(\{l_i^2\}) = \sum_{j \in T} (k \, \epsilon_j - V_j \, \lambda) \,, \tag{5}$$

where $k \equiv 1/8\pi G$ is the inverse Newton's constant and $\lambda \equiv k \, \Lambda/2$ is the redefined cosmological constant.

Dynamical Triangulation

Since in Regge calculus each triangulation T is completely characterized by the set of all squared edge lengths $\{l_i^2\}$, we can in principle carry out the path integral by integrating over all possible edge lengths, i.e., $\int \mathcal{D}g \rightarrow \int \mathcal{D}l$, with each configuration $\{l_i^2\}$ weighted by the corresponding Regge action (5). However, a problem with this approach is that certain triangulations may be over counted due to the gauge freedom in the edge lengths since each edge length is varied continuously. Moreover, one would still like to introduce a suitable cut-off scale for the edge length. Instead, a more restricted version of Regge calculus called dynamical triangulation is employed in CDT.

In dynamical triangulation, one again uses simplicial manifolds and the Regge form of the action, but a different space of triangulated geometries in the path integral. Instead of integrating over all possible edge lengths for a fixed simplicial manifold, one fixed the lengths of the basic simplicial building blocks, and sums over all distinct triangulations of M. It is to be noted that fixing the edge lengths is not a restriction on the metric degrees of freedom since one can still achieve all kinds of deficit angles by appropriate gluing of the
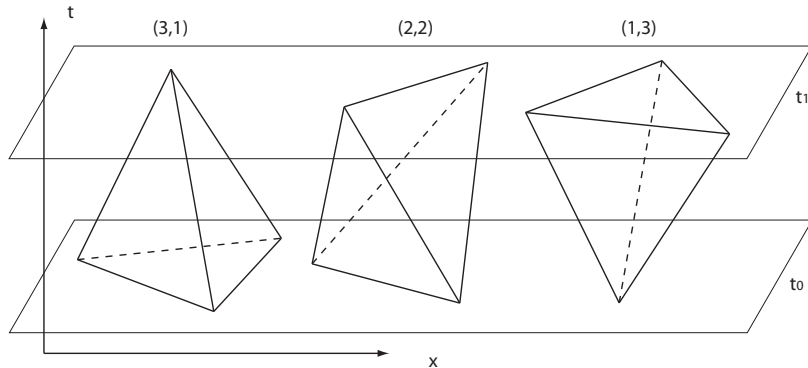
Figure 1: The three types of basic building blocks in three dimensions.

simplicial building blocks. The continuum path integral can thus be written as a discrete sum over inequivalent dynamical triangulations:

$$\int \mathcal{D}g\ e^{iS_{\mathrm{EH}}[g]} \ \rightarrow \ \sum_{T \in \mathcal{T}} \frac{1}{C(T)} e^{iS_{\mathrm{Regge}}(T)}\ , \tag{6}$$

where $1/C(T)$ is the measure on the space of triangulations, with $C(T)$ being the order of the automorphism group of the triangulation T. From a numerical point of view, this is extremely convenient since information about the geometry is reduced to combinatorics, in other words, geometric quantities such as volume and curvature can be obtained by simple counting of the simplicial elements (points, edges, faces, etc.). In addition, an approximation of the path integral can be obtained numerically by sampling the configuration space of all dynamical triangulations (discrete metrics) $\mathcal{T}$. This is exactly what we do in our computer simulations which will be described in detail in section 4.

Role of Causality

Now we are left with the question of how to perform a Wick rotation and explicitly compute the sum in (6). In the old Euclidean dynamical triangulation approach, one makes the substitution $iS_{\mathrm{Lor}} \rightarrow -S_{\mathrm{Euc}}$ and sum over the Euclidean counterparts of the dynamically triangulated Lorentzian geometries, i.e., discrete geometries made up of Euclidean simplicial building blocks. The problem with the Euclidean approach is that the Euclidean geometries that constitute the path integral know nothing about causality, namely the light-cone structure of the spacetime and there is no a priori prescription of how to
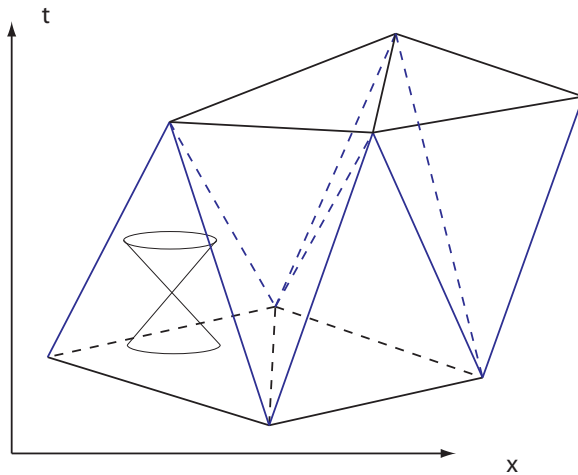
Figure 2: A local subset of a causal dynamical triangulation in three dimensions. Note that each building block tetrahedron has the inherent light-cone structure of a Minkowski space

perform an inverse Wick rotation to recover causality in the full quantum theory. Furthermore, due to the absence of time a large class of highly degenerate geometries contributes to the path integral, causing a well-defined continuum theory fails to exist.

On the contrary, in CDT the causal structure is built into the discrete geometries from the outset. The geometries that are summed over are taken to be the same homeomorphism class, i.e., we do not allow different spacetime topologies to contribute to the path integral. As mentioned before, we will only consider globally hyperbolic simplicial manifolds with a time-foliated structure, where the $(n-1)$-dimensional spatial slices (each labeled by the global time t, not a gauge choice) have a fixed topology (usually taken to be S^{n-1}). In other words, topology changes of the spatial slices are not allowed because spatial topology changes are often associated with causality violation. Each simplicial building block in CDT is taken to be a subset of the Minkowski space together with its inherent light-cone structure. Again, a triangulated geometry along with its global causal structure is obtained by suitable gluing of these simplicial building blocks, each of which has its own local causality, whose spacelike edges all have the same length squared a^2 and whose timelike edges all have the same length squared $-\alpha a^2$, where α denotes an asymmetry factor between the spacelike and timelike geodesic distances. This leaves us

with n types of simplicial building blocks in n dimensions. The three types of building blocks in 3 dimensions are shown in Figure 1. An example of how they are glued together to form a local subset of a 3-dimensional simplicial spacetime is shown in Figure 2.

Wick Rotation and the Euclidean Action

In CDT, Wick rotation is defined by analytical continuation of all timelike edges of each simplicial building block respectively to the Euclidean sector, i.e., by making the substitution $-\alpha a^2 \to \alpha a^2$ for the length square of the timelike edges. This takes a discrete Lorentzian geometry T_{Lor} to its corresponding Euclidean geometry T_{Euc}. As a result, the Lorentzian action is replaced by the corresponding Euclidean action[1], i.e.,

$$iS_{\mathrm{Lor}} \equiv iS_{\mathrm{Regge}}(T_{\mathrm{Lor}}) \;\to\; -S_{\mathrm{Euc}} \equiv iS_{\mathrm{Regge}}(T_{\mathrm{Euc}}) \tag{7}$$

The Wick rotation in effect converts a path integral (a quantum mechanical problem) to a partition function (a statistical mechanical problem). The configuration space of dynamically triangulated spacetimes $\mathcal{T}$ after the Wick rotation can be viewed as a statistical ensemble with the partition function

$$Z = \sum_{T \in \mathcal{T}} e^{-S_{\mathrm{E}}(T)} \,, \tag{8}$$

where $S_{\mathrm{E}}(T)$ is the Euclidean Regge action of the triangulation T. Here we have taken the measure factor $1/C(T)$ to be 1 simply because that based on the general observation in the theory of critical phenomena we do not expect the detailed choice of the measure to affect the continuum limit of the theory. This assumption is further supported by the analytical solution to the CDT model in two dimensions [12]. After rewriting the problem in the language of statistical mechanics, we can readily employ the Monte Carlo method to tackle the problem with computer simulations.

4   Numerical Implementation in 3D

In this section and the rest of the paper, we will only consider the CDT model in three dimensions. Gravity in three dimensions often provides a simpler setting for quantization [13]. For instance, classical 3D gravity is devoid of propagating degrees of freedom. The lower-dimensional theory can serve as an interesting toy model for the study of quantum gravity. In this section, we describe the numerical setup of our simulation.

---

[1]The derivation of this can be found in [11]

Partition Function

It can be shown that in three dimensions and for the special case $\alpha = -1$ (symmetric timelike and spacelike discrete geodesic lengths) the discrete Euclidean action is expressible in terms of the total number of vertices and tetrahedra, N_0 and N_3, in the triangulation T, and takes the form [1]

$$S_{\mathrm{E}}(T) = -k_0 N_0 + k_3 N_3 \,, \tag{9}$$

where

$$\begin{aligned}
k_0 &= \frac{a}{4G} \\
k_3 &= \frac{a^3 \Lambda}{48\sqrt{2}\pi G} + \frac{a}{4G}\left(\frac{3}{\pi}\arccos\frac{1}{3} - 1\right) \,.
\end{aligned} \tag{10}$$

The dimensionless coupling constants k_0 and k_3 will simply be referred to as the inverse Newton's constant and the cosmological constant, respectively. The partition function (8) can thus be written as

$$Z(k_0, k_3) = \sum_{T \in \mathcal{T}} e^{k_0 N_0 - k_3 N_3} \,. \tag{11}$$

One can show that, for finite volume, the model described above is well-defined in the sense of being a statistical system whose transfer matrix is bounded and positive [11].

Data Structure

The particular time-foliated structure of the simplicial manifolds under consideration allows a discretization of the global proper time t. In our simulations, the total number of time intervals is taken to be 8, 16, 32, and 80. For example, in a triangulation with 16 time intervals, each spatial slice is labeled by an integral number between 0 and 16. On the other hand, since each 3-simplex (tetrahedron) sits between two spatial slices, it is labeled with a half-integer.

As already mentioned in the previous section, there are only three types of basic building blocks in three dimensions (Figure 1). We denote each of these building blocks by the number of points it has in the adjacent spatial slices. For instance, the (1,3) simplex has 1 vertex point at t and 3 vertex points at $t + 1$, and so on. The number of (1,3) simplices in the time interval $[t, t + 1]$ will be denoted by $N_{13}(t)$, and likewise for the (2,2) and (3,1) simplices. The following list summarizes the notation we will adopt throughout the remaining paper.

$$
\begin{array}{ll}
N_0 & \text{- number of 0-simplices (points)} \\
N_1 & \text{- number of 1-simplices (edges)} \\
N_2 & \text{- number of 2-simplices (triangles)} \\
N_3 & \text{- number of 3-simplices (tetrahedra)} \\
N_{13} & \text{- number of (1,3) simplices} \\
N_{22} & \text{- number of (2,2) simplices} \\
N_{31} & \text{- number of (3,1) simplices}
\end{array}
$$

Since each triangulated spacetime consists of a set of tetrahedra glued to each other in a specific manner, the data structure we need to deal with in our computer program is not particularly complicated. We use a hash table to store the current configuration during the simulation. Each point in the configuration is labeled by a natural number. In addition, every tetrahedron is assigned an id number which points to a particular entry in the hash table. Each entry in the hash table is a list of numbers that represents the properties of the corresponding tetrahedron. Each list has the structure

$$
(y,\ t,\ p_1,\ p_2,\ p_3,\ p_4,\ n_1,\ n_2,\ n_3,\ n_4)\,, \tag{12}
$$

where y represents the type of the tetrahedron and takes the values 1, 2 or 3 for (1,3), (2,2), or (3,1) simplices, respectively, t is the time at which the tetrahedron resides and assumes half-integer values, the numbers p_1 through p_4 are the labels of the four vertex points, and n_1 through n_4 are the id numbers of the four neighboring tetrahedra that are glued to this tetrahedron (sharing exactly three points). We order the vertex points in the way such that points at the earlier time are placed before the points at the latter time. In addition, the neighboring tetrahedron n_i is glued to the face that does not contain the point p_i. For example, the list $(3, \frac{1}{2}, 1, 2, 3, 4, 10, 11, 12, 13)$ represents a (3,1) simplex at $t = 1/2$ having the vertex points 1, 2, 3, and 4 and are connected to the tetrahedra with id numbers 10, 11, 12, and 13. It can also be inferred from the list that the points 1, 2, and 3 are anchored at $t = 0$ while the point 4 at $t = 1$ as well as the fact that the neighboring tetrahedron 10 shares the triangle 234, and so on.

Monte Carlo Moves

Starting from any initial configuration, the Monte Carlo method generates random configurations by a random walk through the configuration space (in our case, $\mathcal{T}$). Using the technique of detailed balance, we will be able to calculate the expectation value of any observable. Each step in the random

walk is usually referred to as a Monte Carlo move. The computer simulation randomly generates successive Monte Carlo moves and modifies the hash table according to the rules associated with each of the moves.

In three dimensions, there are five basic moves that locally update the triangulation (counting inverse moves as separate). This set of moves is believed to ergodic, that is, any configuration in the ensemble of triangulations can be reached from any other configuration by successive applications of moves from this set. Furthermore, these moves preserve the time-foliation structure as well as the spacetime topology. Note that all of the moves will be rejected if they violate the simplicial manifold property.
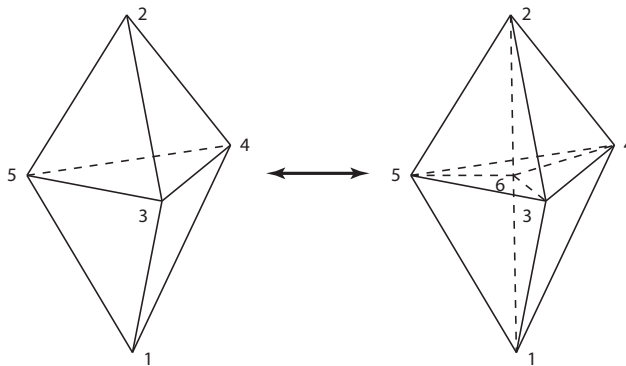
Figure 3: The (2,6) move.
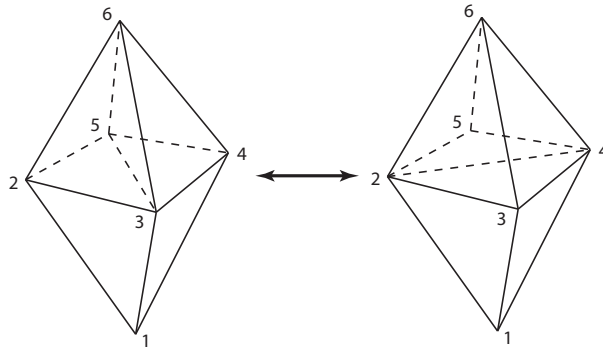
Figure 4: The (4,4) move.

The moves are denoted by a set of two numbers that describe how they locally affect the number of 3-simplices. For example, the (m, n) move is one
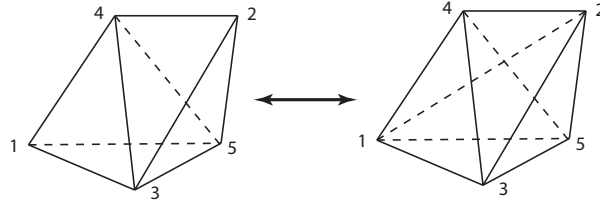
11

Figure 5: The (2,3) move.

that operates on a local subset of m tetrahedra and replaces it by one consisting of n tetrahedra. These moves are illustrated in Figure 3, 4, and 5 where we have also shown the labels of the vertices of the initial and resulting simplices. For instance, the (2,3) move acts on a subset that consists of a (3,1) simplex and a (2,2) simplex sharing one triangular face and turn it into a subset consisting of a (3,1) simplex together with the two other (2,2) simplices. The corresponding inverse move, the (3,2) move, does the exact opposite. Note that the time-reversed version of the above move is also valid. To illustrate explicitly how the moves change the hash table where the information about the triangulation is stored, we show how the lists of a local subset of tetrahedra (with id numbers 1 and 2) are modified by the (2,3) move for the case illustrated in Figure 5:

$$
\begin{align}
1 &: \ (3, \frac{1}{2}, 1, 3, 5, 4, 2, 0, 0, 0) \\
2 &: \ (2, \frac{1}{2}, 3, 5, 4, 2, 0, 0, 0, 1) \\
&\qquad\qquad \Downarrow \\
3 &: \ (3, \frac{1}{2}, 1, 3, 5, 2, 0, 5, 2, 0) \\
4 &: \ (2, \frac{1}{2}, 1, 3, 4, 2, 0, 5, 3, 0) \\
5 &: \ (2, \frac{1}{2}, 1, 5, 2, 4, 0, 4, 0, 3)
\end{align}
\tag{13}
$$

Here 0 simply indicates that the tetrahedron is not connected to any other at that face. A more detailed description of these moves can be found in [11].

Metropolis Algorithm

In order to get sensible, accurate results when simulating statistical systems with a rapidly varying Boltzmann weight (e^{-S_E} in our case), it is vital to use the idea of importance sampling in Monte Carlo integration. The ideal situation is

to sample configurations with a probability given by their Boltzmann weight. Then the Monte Carlo average of N measurements of an observable A would just be

$$\langle A \rangle \equiv \frac{\sum_{T \in \mathcal{T}} A(T) e^{-S_{\mathrm{E}}(T)}}{Z} \approx \frac{1}{N} \sum_{i}^{N} A(C_i) \,, \tag{14}$$

where C_i is the so-called Markov chain of configurations sampled during the simulation. To set up the Markov chain we need to introduce a fictitious dynamics by adjusting the probability of making a transition from one configuration to another based on the change in the Boltzmann weight.

Let $P(C_i)$ be the probability of being in configuration C_i and $W(C_i, C_{i+1})$ be the transition probability of going from C_i to C_{i+1}. The so-called detailed balance condition assures that the random walk reaches an equilibrium probability distribution and is expressed as

$$W(C_i, C_{i+1}) P(C_i) = W(C_{i+1}, C_i) P(C_{i+1}) \,. \tag{15}$$

In terms of the current problem of the statistics of triangulated geometries, the condition is written as

$$\frac{W(T_1, T_2)}{W(T_2, T_1)} = \frac{P(T_2)}{P(T_1)} = \frac{e^{-S_{\mathrm{E}}(T_2)}}{e^{-S_{\mathrm{E}}(T_1)}} = e^{-\Delta S_{\mathrm{E}}} \,. \tag{16}$$

The simplest choice of W that satisfies the detailed balance condition is given by

$$W(T_1, T_2) = \begin{cases} e^{-\Delta S_{\mathrm{E}}} & \text{if } \Delta S_{\mathrm{E}} > 0 \\ 1 & \text{if } \Delta S_{\mathrm{E}} \leq 0 \end{cases} \,. \tag{17}$$

This dynamic method of generating an arbitrary probability distribution is usually referred to as the Metropolis algorithm [14]. According to this condition, each Monte Carlo move is accepted or rejected based on the change in the Euclidean action.

Technical Details of Simulation

In all of our simulations, the spacetime topology is fixed to be $S^1 \times S^2$, where the periodic identification in the time direction has been chosen purely for practical convenience[2]. The strategy for the simulation is the usual one from dynamical triangulations. We first need to fine-tune the bare cosmological

---

[2]We have in fact run our simulation with other boundary conditions. The results have shown be to largely independent of the boundary condition specified.

constant to its critical value $k_3^c(k_0)$. As we know from the study of Euclidean simplicial quantum gravity, one can hope to obtain a continuum limit for the discretized gravity by taking the limit $k_3 \to k_3^c(k_0)$. Note that the critical value k_3^c depends on the value of the bare inverse gravitational coupling k_0 (Figure 6).
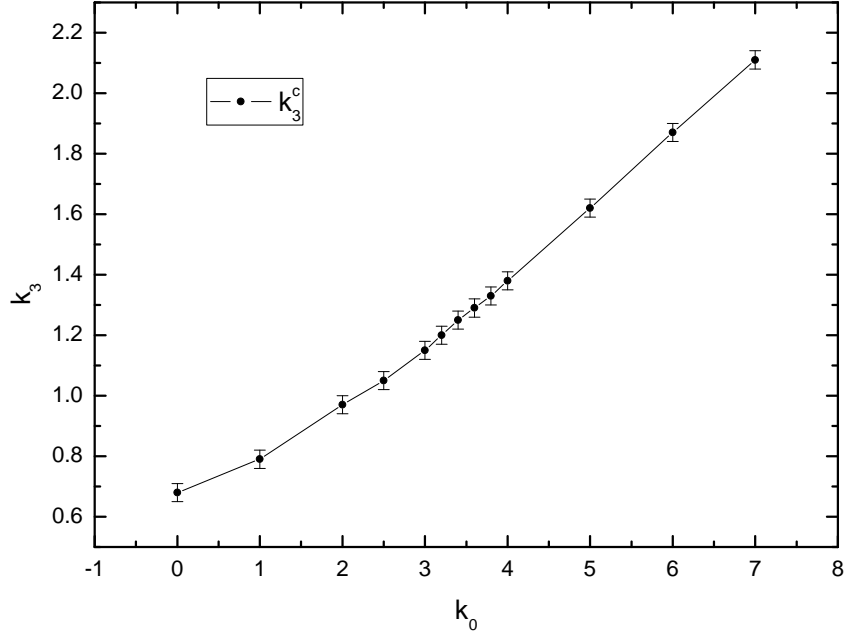

Figure 6: The critical value of k_3 as a function of k_0.

The model described thus far is based on a grand canonical ensemble, since the nature of the set of Monte Carlo moves used in the simulation allows the total spacetime volume N_3 to vary. For convenience, we will instead simulate a canonical ensemble with a fixed volume N_3 by adjusting the coupling constant k_3 to its critical value. Near the critical value k_3^c, the fluctuations of spacetime volume are bounded within a certain range. To make sure that the volume is peaked at a prescribed value V, with a well-defined range of fluctuations, we add to the action (9) an extra term

$$\delta S = \epsilon |N_3 - V| , \tag{18}$$

where ϵ controls the range of fluctuation and is taken to be 0.02 in all of our simulations.

We then calculate the expectation values of suitable observables for these dynamically generated quantum spacetimes, according to formula 14. We
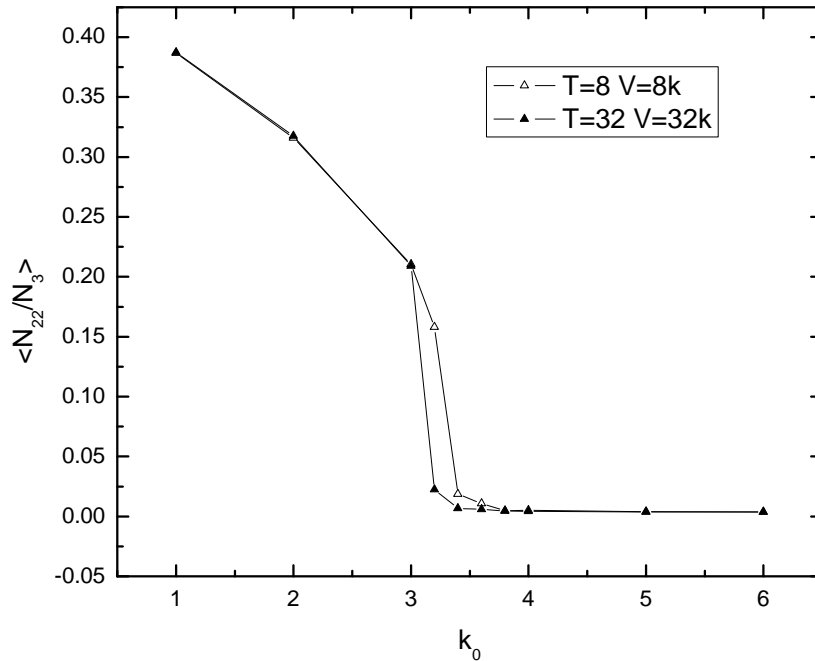
Figure 7: The value of the order parameter N_{22}/N_3 as a function of the inverse Newton's constant k_0.

have performed the simulation for systems sizes of $V = 8k$, 16k, 32k, and 50k tetrahedra. One sweep of the system is defined as V attempted moves. We construct our initial configuration by taking a spherically symmetric spatial triangulation and translate it in the time direction. Before any measurements are taken, the systems needs to be thermalized so that the artificial initial configuration is "forgotten". We usually take the themalization to be about 10^5 sweeps. During the simulation, measurements are made at every 100 sweeps.

5   Results of Computer Simulation

In this section we will analyze data coming from our numerical studies of three-dimensional causal dynamical triangulation of quantum gravity.

Phase Structure

We first run our Monte Carlo simulation with different values of k_0 (from 1.0 to 6.0) to explore the phase space of our system. We use the ratio between

the total number of (2,2) simplices N_{22} and the total spacetime volume N_3 as an order parameter. Figure 7 shows the expectation value of the ratio N_{22}/N_3 as a function of the coupling constant k_0 for two different types of spacetime configuration. We observe a phase transition at the critical value k_0^c of about 3.3.
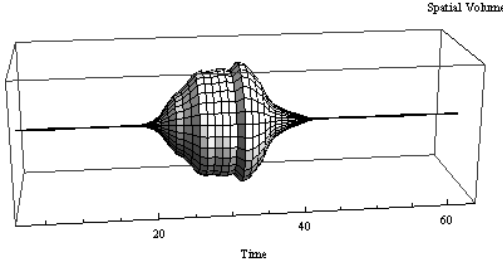

Figure 8: A Monte Carlo snapshot in the phase for $k_0 < k_0^c$
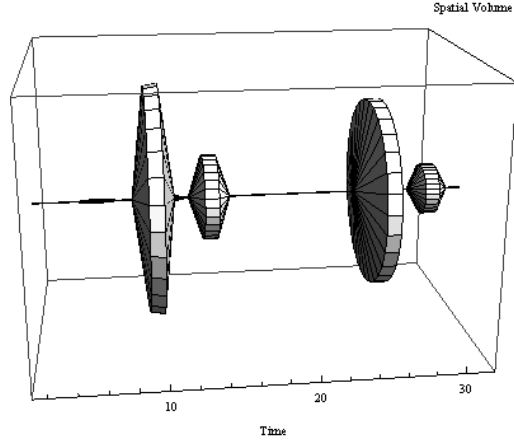
Figure 9: A Monte Carlo snapshot in the phase for $k_0 > k_0^c$

In the phase where $k_0 > k_0^c$, the spatial volumes of successive spatial slices become decoupled. A typical snapshot of the spacetime geometry during the computer simulation is shown in Figure 9 where we plot the spatial volume N_2 as a function of time t. Note that the plot is rotated around the time axis for better visualization; it does not mean that the spacetime is axial-symmetric. We notice from the plot that in this phase, the spatial volume can change from essentially zero to a macroscopic size in one time-step, suggesting that there is no correlation between spatial volumes separated by more than a few time-steps. In fact, in this phase, the 3D CDT model can be viewed as a product of uncoupled 2D Euclidean models and is thus not relevant to the 3D theory of gravity.

On the other hand, in the phase where $k_0 < k_0^c$, we observe the emergence of a well-behaved extended geometry from our simulation as suggested by a typical snapshot for $k_0 = 2.0$ shown in Figure 8. After a sufficient number of Monte Carlo moves (typically about 100k sweeps), the system reaches a configuration that fluctuates around an extended "ground state" geometry, one that resembles a classical universe. It is to be noted that we have at no stage specified a preferred background geometry. In this phase, the volumes of successive spatial slices are strongly coupled. In fact, we will calculate the
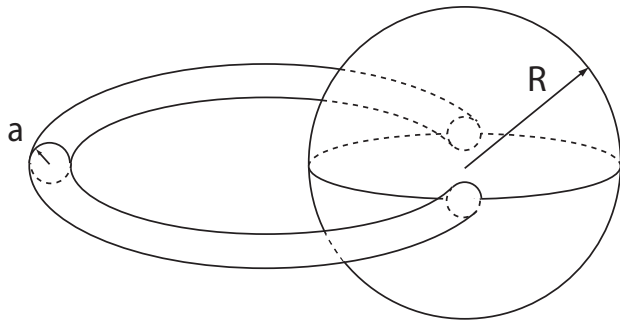
16

Figure 10: An illustration of the nearly classical universe described in the text.

volume-volume correlation function which is a coordinate invariant measure of how much the volumes of two spatial slices are correlated as a function of the separation in time and compare it to the correlation function of a nearly classical solution. The close resemblance of the two correlation functions justifies our calling the geometry that emerges from our simulation the "ground state" geometry. In the rest of the paper, we will only discuss the physical properties of the model in this phase, with $k_0 = 2.0$.

Extended Ground State Geometry

For a compact topology, the simplest solution to the Einstein's equations with a Euclidean signature and a positive cosmological constant is the symmetric 3-sphere. We can adapt the S^3 solution to the $S^1 \times S^2$ topology at hand by cutting away two open balls at the two opposite ends of the S^3 geometry and attaching a thin cylinder $I \times S^2$ of radius a at the cut-off scale to the two ends. The resulting geometry is very close to a solution to Einstein's equations in the sense that the contribution to the path integral from the cylindrical part is negligible. A schematic illustration of this geometry is shown in Figure 10.

The correlation function for the discrete geometry is given by the formula below.

$$C(\Delta) = \frac{1}{T^2} \sum_{t=1}^{T} \langle N_2(t) N_2(t + \Delta) \rangle \tag{19}$$

As seen from the above formula, the correlation function is translation invariant in time and is calculated by averaging over independent configurations sampled during the simulation. To calculate the correlation function of the "nearly classical" solution, we use instead a continuous version (without the
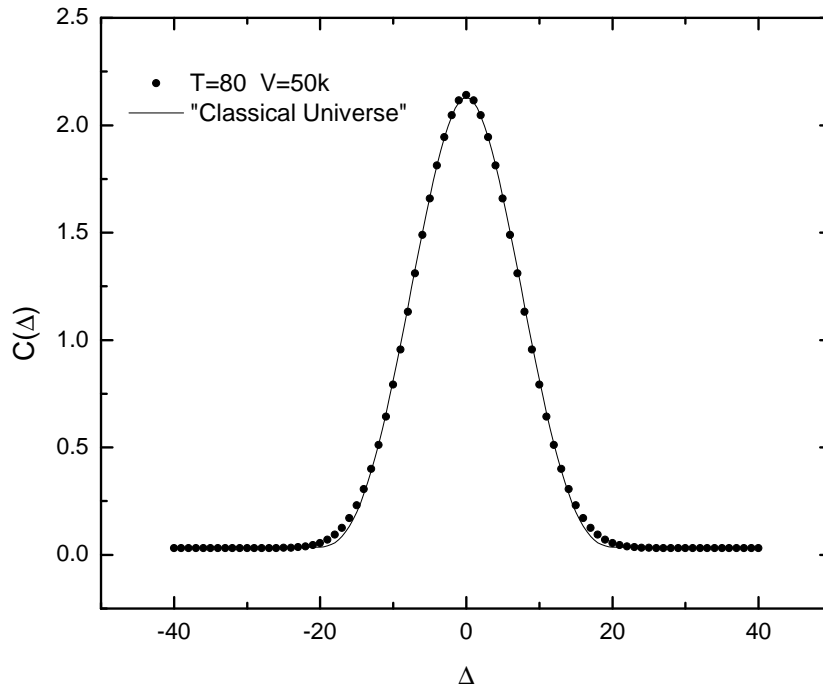
Figure 11: The correlation function. The dotted plot is the measured correlation function of the system of size $T = 80$ and $V = 50k$. The continuous curve corresponds to the nearly classical solution described in the text

averaging) of the above formula:

$$C(\Delta) = \frac{1}{T^2} \int_1^T dt N_2(t) N_2(t + \Delta) \,. \qquad (20)$$

Figure 11 shows the correlation functions, where the dots represent the measured values for a spacetime with total time $T = 80$ and total spacetime volume $V = 50k$ and the continuous curve corresponds to the "nearly classical" solution. We have adjusted the radius R of the 3-sphere and the radius a of the cylinder as free parameters to produce a nice fit through the measured values. The result indicates that the universe that emerges from the simulation indeed behaves semi-classically, at least as far as macroscopic geometric properties are concerned.

Spectral Dimension

To further demonstrate that our simulation in fact produces a semi-classical universe, we have also measured the effective dimension by superimposing a

diffusion process on the discretized geometric ensemble. The method is described in detail in [15]. The basic idea is to perform a random walk in a given spacetime configuration after the Monte Carlo simulation has thermalized. Starting from any tetrahedron, a random path is generated by randomly walking to one of the four neighboring tetrahedra at each successive step. From a large number of random paths of σ steps, one can extrapolate the return probability $P(\sigma)$, namely the probability of a random walk that starts and ends at the same tetrahedron in σ steps. Since we are interested in the region of spacetime with extended spatial volume, we will only start the random walks on the spatial slice with the maximal spatial volume. Moreover, we average over the return probabilities obtained with different starting tetrahedra and on independent spacetime configurations generated in the Monte Carlo simulation.

The return probability for diffusion on fractal geometry is well-studied and is given by the formula

$$P(\sigma) \approx \sigma^{-D/2}\,, \tag{21}$$

when the diffusion time is considerably smaller than $N_3^{2/D}$. Here D is the so-called spectral dimension, which is not necessarily an integer. The spectral dimension can be extracted from the return probability by taking the logarithmic derivative if the finite-size correction is neglected, i.e.,

$$D(\sigma) = -2\frac{d\log P(\sigma)}{d\log \sigma} + \text{finite-size correction.} \tag{22}$$

The result for the measurements of the spectral dimension is shown in Figure 12. The following table lists the system sizes we work with and the number of sweeps we perform before the measurement of spectral dimension.

T	V	# of sweeps
32	16k	200k
64	32k	180k
80	50k	100k

We first notice that at sufficiently large σ, the finite-size effect takes over and drives the dimensionality down. This is particularly apparent for the system with the smallest volume. Based on similar work in four dimensions [3] we expect that the dimensionality should approach the value 3 at large σ for our 3D model before the finite-size effect becomes dominant. However, the measured dimensionality of the extended ground state universe overpasses 3 at σ values beyond 150. We speculate that this may be due to the fact that the
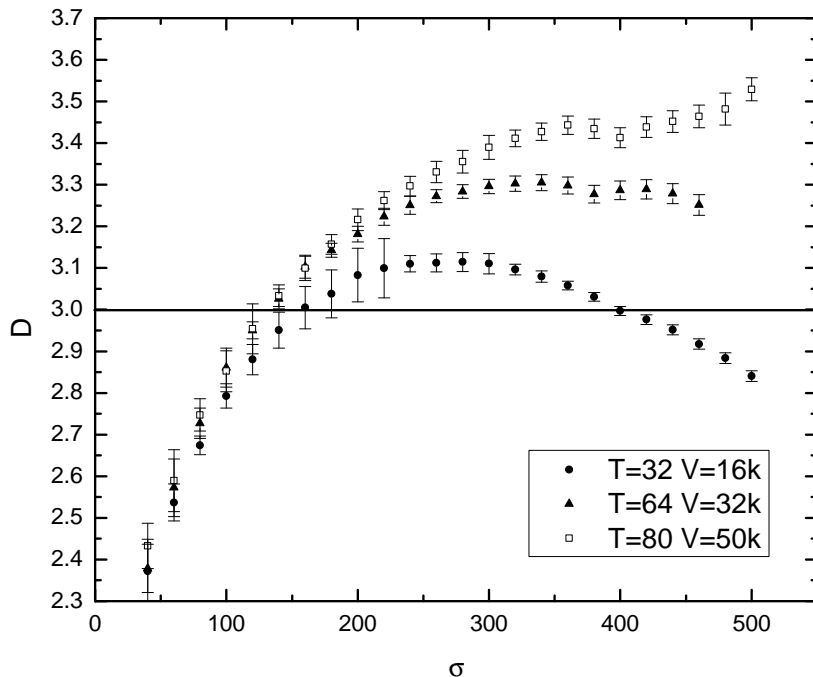
Figure 12: The spectral dimension as a function of the diffusion time σ, measured for three different system sizes.

systems under investigation have not reached adequate thermalization during the Monte Carlo simulation so that even though the macroscopic geometric properties such as spatial volume exhibits a classical behavior, more detailed geometric structure still does not resemble that of a three-dimensional classical spacetime.

The number of steps or equivalently the diffusion time σ is a good characterization of the length scales at which we are probing the spacetime. We observe that at small scales ($\sigma < 100$) the dimensionality is considerably smaller than 3 which we believe is an indication of the highly non-classical behavior at small length scales. This is an evidence that, microscopically, the geometry is dominated by random quantum fluctuation so that the classical notion of dimensionality becomes impertinent. We also believe that with sufficient thermalization and a large enough volume, the dimensionality should approach 3 for large σ to exhibit the smooth three-dimensional classical spacetime at large length scales. For the case with spacetime volume of 16k and 200k sweeps, which is the most thermalized among the three systems we have studied, we indeed observe that the measured spectral dimension is nearly 3 before the finite-size effect takes over at $\sigma \approx 300$. Measurements of spectral dimension

on more thermalized systems are currently in progress. There is hope that a more accurate measurement will yield the result that the dimensionality approaches the value 3 asymptotically for increasing σ and will also allow us to extrapolate the behavior of the dimensionality in the limit as $\sigma \to 0$.

6   Conclusion

In sum, our numerical simulation of the three-dimensional CDT model has produced results in agreement with the results obtained by Loll, and etc. A well-behaved extended ground state universe emerges dynamically in the Monte Carlo simulation. For the first time, measurements of the spectral dimension of the emergent universe are conducted on a 3D CDT model. A scale dependence of the spectral dimension is also observed. A more precise measurement of the spectral dimension will hopefully yield more persuasive results for the behavior of the dimensionality in the limit of large and small length scales.

This project provides a basis for further work on CDT in three dimensions. There are a number of generalizations to the model that are interesting to study. In our simulations, we have restricted the spatial topology to be that of S^2. In the future, we can adapt the model to spaces of torus topology and compare the results to analytical solutions based on other approaches to quantum gravity. We can also examine the effects of matter fields (ex. a scalar boson ϕ) coupled to gravity.

7   Acknowledgments

References

[1] J. Ambjørn, J. Jurkiewicz and R. Loll, *Non-perturbative 3d Lorentzian quantum gravity*, Phys. Rev. D 64 044011, (2001), [arXiv:hep-th/0105267].

[2] J. Ambjørn, J. Jurkiewicz and R. Loll, *Emergence of a 4D world from causal quantum gravity*, Phys. Rev. Lett. 93 (2004) 131301 [arXiv:hep-th/0404156].

[3] J. Ambjørn, J. Jurkiewicz and R. Loll, *Spectral dimension of the universe*, Phys. Rev. Lett. 95 (2005) 171301 [arXiv:hep-th/0505113].

[4] R. M. Wald, *General Relativity*, (The University of Chicago Press, 1984).

[5] R. P. Feynman and A. R. Hibbs, *Quantum Physics and Path Integrals*, (McGraw-Hill, 1965).

[6] J. Ambjørn, J. Jurkiewicz and R. Loll, *The universe from scratch*, Contemp. Phys. 47 (2006) 103-117 [arXiv:hep-th/0509010].

[7] J. Ambjørn and J. Jurkiewicz, *Four-dimensional simplicial quantum gravity*, Physics Letters B 278 42-50, (1992).

[8] T. Regge, *General relativity without coordinates*, Nuovo Cim. 19: 558-571, (1961).

[9] R. M. Williams and P. A. Tuckey, *Regge calculus: a brief review and bibliography*, Class. Quant. Grav. 9: 1409-1422, (1992).

[10] C. W. Misner, K. S. Thorne, J. A. Wheeler, *Gravitation*, (W. H. Freeman, 1973).

[11] J. Ambjørn, J. Jurkiewicz and R. Loll, *Dynamically triangulating Lorentzian quantum gravity*, Nucl. Phys. B 610 347-382, (2001), [arXiv:hep-th/0105267].

[12] J. Ambjørn and R. Loll, *Non-perturbative Lorentzian quantum gravity, causality and topology change*, Nucl. Phys. B 536 407-434, (1998), [arXiv:hep-th/9805108].

[13] S. Carlip, *Quantum Gravity in 2+1 Dimensions*, (Cambridge University Press, 1998).

[14] N. Metropolis, A.W. Rosenbluth, M.N. Rosenbluth, A.H. Teller, and E. Teller. *Equations of State Calculations by Fast Computing Machines.* Journal of Chemical Physics, 21(6): 1087-1092, (1953).

[15] J. Ambjørn, J. Jurkiewicz and R. Loll, *Reconstructing the universe*, Phys. Rev. D 72 (2005) 064014 [arXiv:hep-th/0505154].